Experimental and Simulation Results for the Removal of H2S from Biogas by Means of Sodium Hydroxide in Structured Packed Columns

Hamadi Cherif, Christophe Coquelet, Paolo Stringari, Denis Clodic, Laura Pellegrini, Stefania Moioli, Stefano Langé

Experimental and Simulation Results for the Removal of H_2S from Biogas by Means of Sodium Hydroxide in Structured Packed Columns

Hamadi Cherif, Christophe Coquelet, Paolo Stringari, Denis Clodic, Laura Pellegrini, Stefania Moioli, Stefano Langè

Abstract—Biogas is a promising technology which can be used as a vehicle fuel, for heat and electricity production, or injected in the national gas grid. It is storable, transportable, not intermittent and substitutable for fossil fuels. This gas produced from the wastewater treatment by degradation of organic matter under anaerobic conditions is mainly composed of methane and carbon dioxide. To be used as a renewable fuel, biogas, whose energy comes only from methane, must be purified from carbon dioxide and other impurities such as water vapor, siloxanes and hydrogen sulfide. Purification of biogas for this application particularly requires the removal of hydrogen sulfide, which negatively affects the operation and viability of equipment especially pumps, heat exchangers and pipes, causing their corrosion. Several methods are available to eliminate hydrogen sulfide from biogas. Herein, reactive absorption in structured packed column by means of chemical absorption in aqueous sodium hydroxide solutions is considered. This study is based on simulations using Aspen Plus™ V8.0, and comparisons are done with data from an industrial pilot plant treating 85 Nm^3/h of biogas which contains about 30 ppm of hydrogen sulfide. The rate-based model approach has been used for simulations in order to determine the efficiencies of separation for different operating conditions. To describe vapor-liquid equilibrium, a γ/ϕ approach has been considered: the Electrolyte NRTL model has been adopted to represent non-idealities in the liquid phase, while the Redlich-Kwong equation of state has been used for the vapor phase. In order to validate the thermodynamic model, Henry's law constants of each compound in water have been verified against experimental data. Default values available in Aspen Plus™ V8.0 for the properties of pure components properties as heat capacity, density, viscosity and surface tension have also been verified. The obtained results for physical and chemical properties are in a good agreement with experimental data. Reactions involved in the process have been studied rigorously. Equilibrium constants for equilibrium reactions and the reaction rate constant for the kinetically controlled reaction between carbon dioxide and the hydroxide ion have been checked. Results of simulations of the pilot plant purification section show the influence of low temperatures, concentration of sodium hydroxide and hydrodynamic parameters on the selective absorption of hydrogen sulfide. These results show an acceptable degree of accuracy when compared with the experimental data obtained from the pilot plant. Results show also the great efficiency of sodium hydroxide for the removal of hydrogen sulfide. The content of this compound in the gas leaving the column is under 1 ppm.

Keywords—Biogas, hydrogen sulfide, reactive absorption, sodium hydroxide, structured packed column.

I. INTRODUCTION

RECENT decades were accompanied by economic growth and prosperity for humanity. This growth gained from oil and natural gas production has been accompanied by an environmental pollution that may trigger irreversible changes in the environment with catastrophic consequences for humans. Moreover, issues related to the reduction of fossil reserves are still relevant, and the global primary energy demand is increasing, pushing the international community to pursue the development of renewable energies.

Among renewable energies, biogas is a possibility. Generally, this gas composed of methane and carbon dioxide, also contains other compounds as water, ammonia, volatile organic compounds and hydrogen sulfide.

Biogas can be valued in several applications such as production of heat and/or electricity, feed for fuel cells, injection into the natural gas grid and production of liquefied bio-methane. This last application presents an environmental and economic benefit. Liquefied bio-methane is the best fuel for the reduction of carbon dioxide emissions with a reduction potential up to 97 % compared to Diesel. It can effectively reduce emissions of greenhouse gases and the pollution, responsible for 42,000 premature deaths annually in France [1].

Liquefied bio-methane requires very low temperatures which may lead to solidification of impurities and thus facilities malfunctions. These impurities must be separated from the biogas. This implies implementation of a purification process to remove from the raw biogas all unwanted substances in order to maximize its methane content. In particular, the complete desulfurization of biogas is peremptory in order to ensure an optimal operation and a high purity of other compounds to valorize, such as carbon dioxide. Moreover, the presence of hydrogen sulfide in the wet biogas, is a poison for installations. Hence, the need to remove all traces of this compound.

The aim of this work is to simulate reactive absorption in structured packed column for the removal of hydrogen sulfide

Hamadi Cherif is with the Mines Paris Tech, PSL, Research University, CTP- Centre des Thermodynamiques des Procédés - Département Énergétique et Procédés, 35 rue St Honoré 77305 Fontainebleau, France and CryoPur R&D society, 3, Rue de la croix martre, 91120 Palaiseau, France (e-mail: hamadi.cherif@mines-paristech.fr).

Christophe Coquelet, and Paolo Stringari are with the Mines ParisTech, PSL, Research University, CTP - Centre des Thermodynamiques des Procédés - Département Énergétique et Procédés, 35 rue St Honoré 77305 Fontainebleau, France.

Denis Clodic is with the CryoPur R&D society, 3, Rue de la croix martre, 91120 Palaiseau, France.

Laura Pellegrini, Stefania Moioli, Stefano Langè are with the GASP – Group on Advanced Separation Processes & Gas Processing, Dipartimento di Chimica, Materiali e Ingegneria Chimica "G. Natta" P.zza Leonardo da Vinci, 32, 20133 Milano, Italy.

by means of sodium hydroxide using Aspen Plus™ V8.0. The obtained results are compared to experimental data from an industrial pilot plant.

II. EXPERIMENTAL

Experiments were performed on a pilot plant "BioGNVAL" treating 85 Nm³/h of biogas from the treatment of sewage sludge. It uses a cryogenic method to purify and liquefy biogas efficiently without loss of methane and without emitting greenhouse gases.

The system generates two products from biogas: liquid bio-methane and bioCO₂ at purity level greater than 99.995 %. [2] This latter requirement needs the removal of all traces of H₂S

in biogas. To ensure this performance, reactive absorption technology is used. It combines two unit operations in one: absorption based on the transfer of the pollutant in the liquid phase and its degradation by a chemical reaction using an aqueous solution of sodium hydroxide. Knowing that biogas contains about 30 ppm of H₂S at the inlet of the pilot plant, the selected method should reduce its content to less than 1 ppm.

The operating principle of reactive absorption is simple. The system mainly comprises a structured packed column, a water circuit and two heat exchangers, used to cool biogas and the liquid phase. Fig. 1 shows the apparatus setup for the desulfurization process.
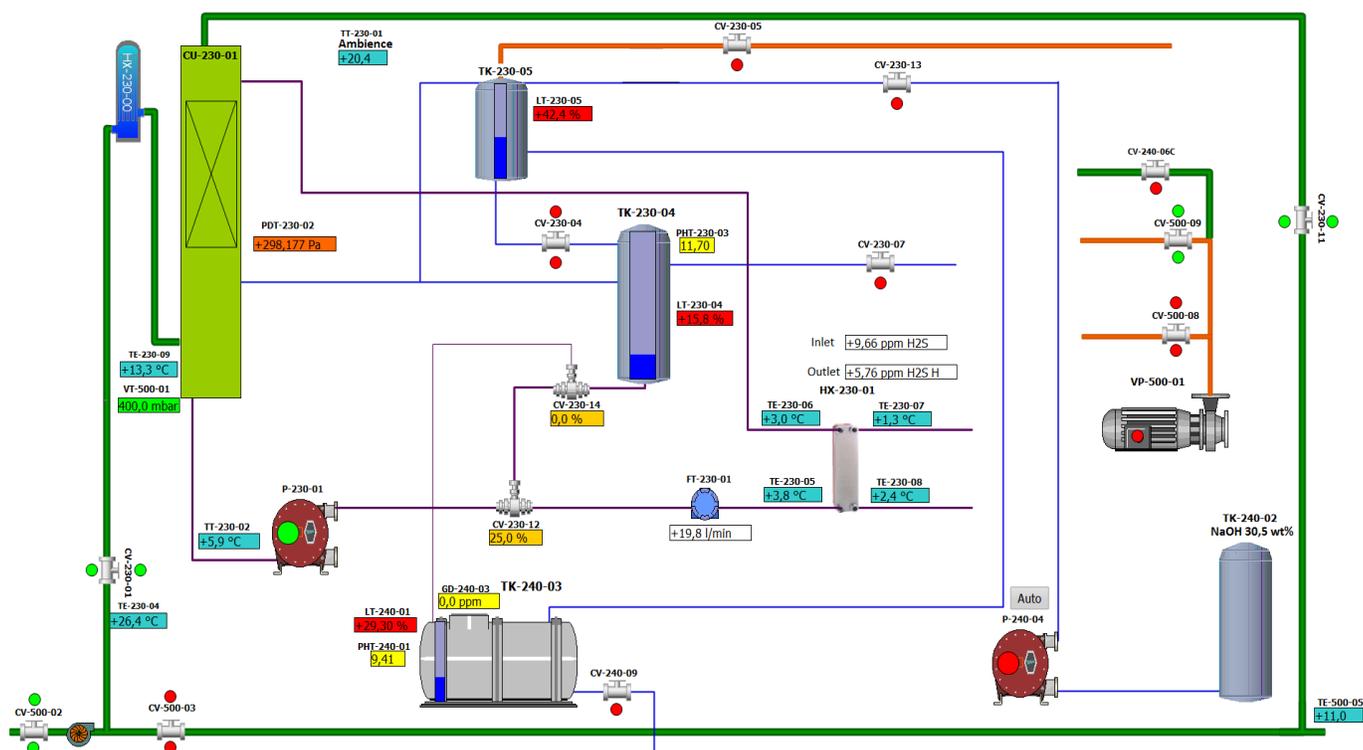

Fig. 1 Schematic diagram of the system for elimination of hydrogen sulfide [3]

Biogas firstly passes through a heat exchanger to cool the gas phase and condense a portion of the water vapor contained therein.

A phase separator recovers the condensed water vapor and sends it to a drainage tank. Thereafter, the biogas enters the bottom of the absorption column where it is contacted in a counter-current with the washing water sprayed from the top. This water is neutralized by an aqueous solution of sodium hydroxide. The injected quantity is controlled by a pH meter placed on the tank *TK-230-04*. This tank showed in Fig. 1 provides the column with the liquid phase.

The liquid phase is recirculated by a pump and is cooled by an exchanger to a temperature slightly higher than 2°C to prevent freezing. Biogas finally exits from the top of the column at a temperature of about 4°C. The cooling duty is provided by the liquid phase on the surface of the packing in direct contact within the column. High efficient mass and heat

transfer between the liquid and the biogas are achieved thanks to the packing surface.

When hydrogen sulfide is absorbed into a sodium hydroxide solution, it can react directly with hydroxyl ions by a proton transfer reaction as seen in reaction R.6 (Section III *F)*. Compared to the diffusion phenomena, this reaction is extremely rapid and can be considered instantaneous. Since hydrogen sulfide is absorbed more rapidly than carbon dioxide by aqueous sodium hydroxide solutions, partial selectivity can be attained when both gases are present. Selectivity is favored by short gas-liquid contact times and low temperatures. [4]

III. ASPEN PLUS™ SIMULATIONS

The aim of these simulations in Aspen Plus™ V8.0 is to study realistically the effectiveness of a structured packed column which uses sodium hydroxide as a chemical solvent for the selective removal of hydrogen sulfide.

Unlike amines, sodium hydroxide is not regenerable but it is very effective in removing low contents of H_2S [4]. Although the liquid solution is recycled, experimental data showed that the NaOH consumption is quite constant. NaOH concentration can be assumed to be constant over time in the liquid phase. This assumption justifies the use of the model "Rate-based" for the study. The rate-based modeling approach is realistic compared to the traditional equilibrium-stage modeling approach that has been employed extensively in the process industries over the decades. The rate-based models assume that separation is caused by mass transfer between the contacting phases, and use the Maxwell-Stefan theory to calculate mass transfer rates [5]. Conversely, the equilibrium-stage models assume that the contacting phases are in equilibrium with each other, which is an inherent approximation because the contacting phases are never in equilibrium in a real column.

TABLE I
COEFFICIENTS USED BY ASPEN PLUS™ TO CALCULATE HENRY'S CONSTANTS

Component i	CH_4	CO_2	H_2S
Component j	H_2O	H_2O	H_2O
Low temperature [°C]	1.85	-0.15	-0.15
High temperature [°C]	79.85	226.85	149.85
a_{ij}	183.7811	159.1997	346.625
b_{ij}	-9111.67	-8477.711	-13236.8
c_{ij}	-25.0379	-21.957	-55.0551
d_{ij}	0.0001434	0.00578	0.05957
e_{ij}	0	0	0

The rate-based modeling approach has many advantages over the equilibrium-stage modeling approach. The rate-based models represent a higher fidelity, more realistic modeling approach and the simulation results are more accurate than those attainable from the equilibrium-stage models [6].

In order to develop a rigorous and thermodynamically consistent simulation, the generalized electrolyte Non-Random Two-Liquid (ENRTL) model proposed by Chen and Song [7] is used for calculating the liquid phase properties, while the Redlich-Kwong equation of state is used to calculate the vapor phase properties. In calculating the non-symmetric activity coefficients of the solutes, the infinite dilution activity coefficients will be calculated based on infinite-dilution condition in pure water, instead of in mixed solvents. This model is verified and validated using various experimental data from literature.

A. Validation of the Temperature-Dependent Henry's Constant for $CH_4 - H_2O$, $CO_2 - H_2O$ and $H_2S - H_2O$ Systems

CH_4, CO_2 and H_2S are selected as Henry-components to which Henry's law is applied and the Henry's constants are retrieved from Aspen Plus databanks for these components with water. Henry's constants are based on the mole fraction scale. The temperature dependence of the Henry's constants used by Aspen Plus™ is represented by:

$$\ln H_{ij} = a_{ij} + \frac{b_{ij}}{T} + c_{ij} \ln T + d_{ij} T + \frac{e_{ij}}{T^2} \qquad (1)$$

Coefficients a_{ij}, b_{ij}, c_{ij}, d_{ij} and e_{ij} for each system are summarized in Table I. Henry's constants obtained with Aspen Plus™ were compared to experimental data from the research report 48 of the Gas processors Association [8]. Results of Henry's constants were also compared to the semi-empirical equation proposed by Harvey [9].

$$\ln H_{ij} = \ln P_{s,j} - \frac{a_{ij}}{T^*} + b_{ij} \frac{\left(1 - T^*\right)^{0.355}}{T^*} + c_{ij} e^{1-T^*} T^{*(-0.41)} \qquad (2)$$

where $P_{s,j}$ is the vapor pressure of the component j, and T^* is the reduced temperature. They are calculated respectively using (3) and (4):

$$P_{s,water} = \exp(73.649 - \frac{7258.2}{T} - 7.3037 \ln T + 4.1653.10^{-6} T^2) \quad (3)$$

$$T^* = \frac{T}{T_{c,eau}} \qquad (4)$$

where $T_{c,eau}$ is the critical temperature of water. Coefficients a_{ij}, b_{ij} and c_{ij} used by Harvey [9] in (2) are summarized in Table II for each system.

TABLE II
COEFFICIENTS USED BY HARVEY TO CALCULATE HENRY'S CONSTANTS

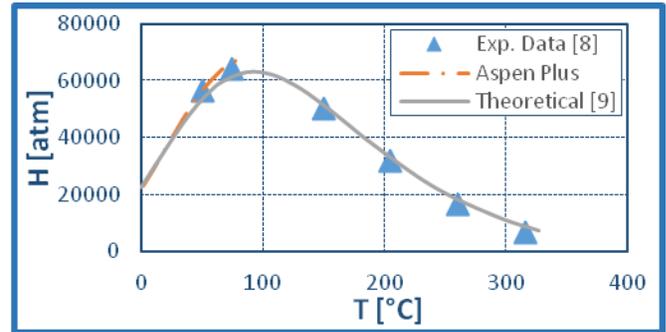| Component i	CH_4	CO_2	H_2S
Component j	H_2O	H_2O	H_2O
a_{ij}	11.01	9.4234	5.7131
b_{ij}	4.836	4	5.3727
c_{ij}	12.52	10.32	5.4227

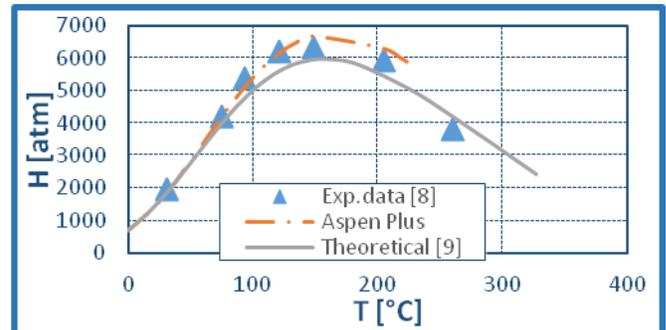Fig. 2 Henry coefficients for CH_4 - H_2O system

Fig. 3 Henry coefficients for CO_2 - H_2O system

The obtained results are similar, with no major differences. Figs. 2-4 show the adequacy of the results for the systems CH_4 - H_2O, CO_2 - H_2O and H_2S - H_2O respectively. The average absolute deviation is equal to 1.2% for CH_4 – H_2O system, 1.9 for CO_2 – H_2O system and 7.8% for H_2S – H_2O system.
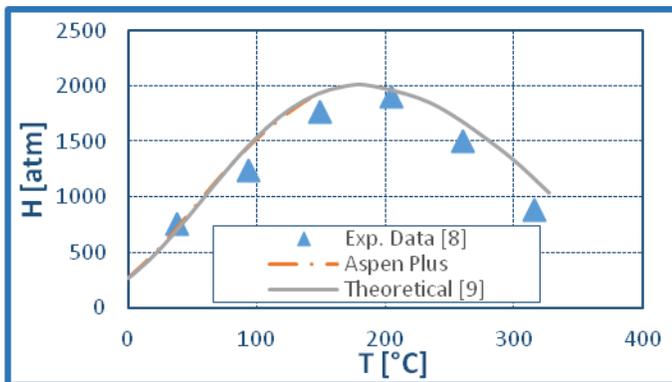

Fig. 4 Henry coefficients for H_2S - H_2O system

B. Validation of Heat Capacity for Carbon Dioxide

Some physical properties as heat capacities of pure components used for heat and mass transfer modelling were checked. Fig. 5 shows for example the comparison of results obtained with the adopted model in Aspen Plus™ with experimental data [10]. The average absolute deviation is equal to 1.85%.
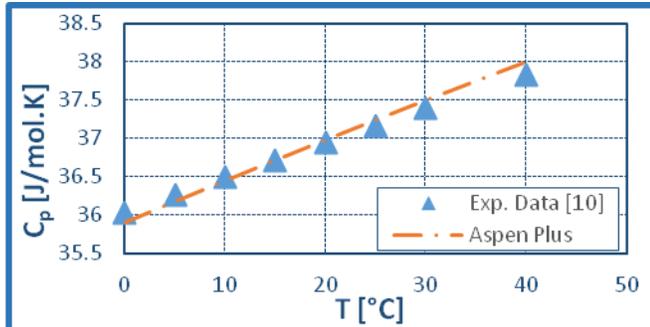

Fig. 5 Comparison between model and experimental data for heat capacity for carbon dioxide
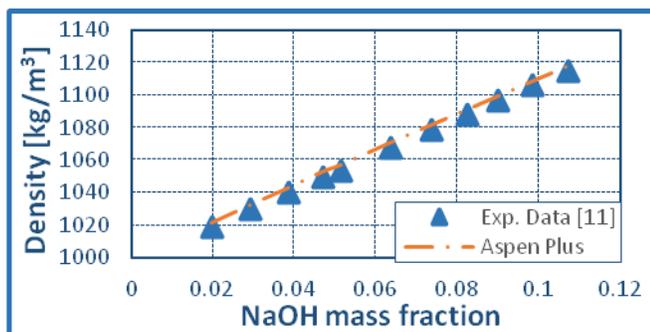

Fig. 6 Comparison between model and experimental data for liquid density of NaOH – H_2O

C. Validation of Liquid Density of NaOH – H_2O

The calculations of the density of the liquid phase have been verified depending on the mass fraction of sodium hydroxide at 25°C. The results obtained with Aspen Plus ™ are in good agreement with experimental data [11] as shown in Fig. 6. The average absolute deviation is equal to 0.3%.

D. Validation of Liquid Viscosity of NaOH – H_2O

For the liquid viscosity, a corrective model for electrolytes called "Jones-Dole" is applied in Aspen Plus™. This model uses the mass fraction of the solvent in the liquid phase. When the weight percentage of NaOH in the liquid phase exceeds 10%, Aspen Plus™ uses the equation of Breslau and Miller instead of that of Jones and Dole.

The electrolyte correction model parameters were improved for the ion HCO_3^- using $KHCO_3$ - H_2O viscosity data [12]. For ion CO_3^{2-}, parameters have been optimized considering experimental data for the K_2CO_3 - H_2O system [13].

The regression of parameters for Na^+ ion was performed with viscosity data of NaOH – H_2O system [14]. For other ions, values provided by Aspen Plus™ database were used.

Fig. 7 shows the fit between experimental data and Aspen Plus™ results for the viscosity of the liquid phase as a function of the mass fraction of sodium hydroxide. Data of this comparison are carried out at a temperature of about 25°C. Knowing that the weight percentage of sodium hydroxide used for simulations does not exceed 10%, the deviation between the results in this range is inferior to 1.9%.
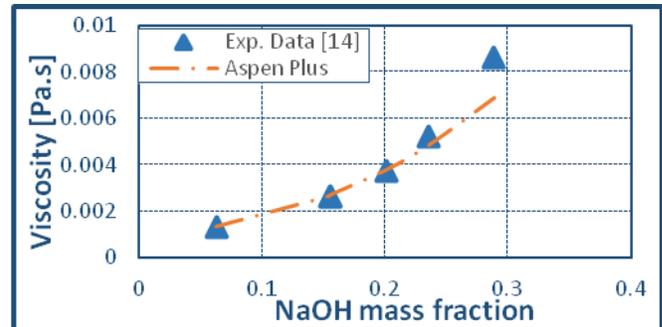

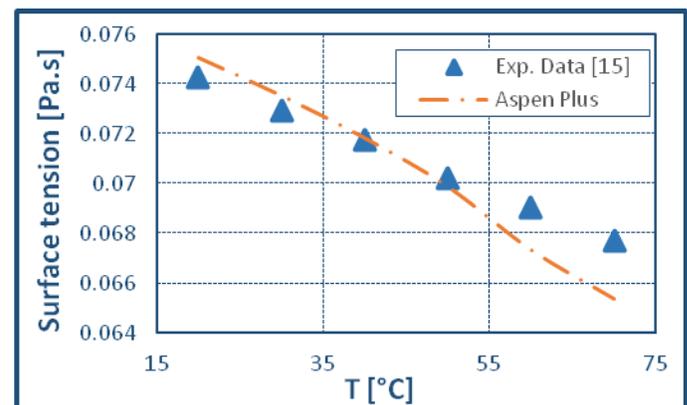Fig. 7 Comparison between model and experimental data for liquid viscosity of NaOH – H_2O

Fig. 8 Comparison between model and experimental data for liquid phase surface tension of 5 wt% NaOH aqueous solution

The average absolute deviation in the entire interval is equal to 5.3%.

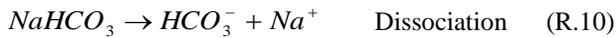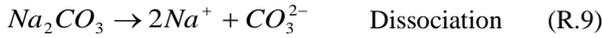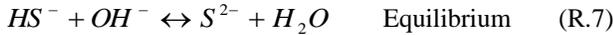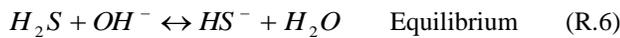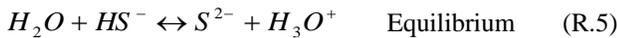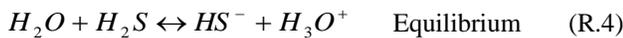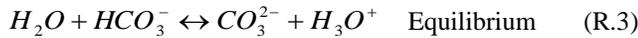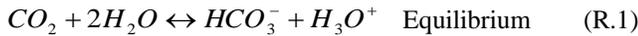*E. Validation of Surface Tension of NaOH – H₂O*

To calculate the liquid phase surface tension, Aspen Plus™ uses the model of Onsager-Samaras. Results obtained were compared to experimental data found in literature as shown in Fig. 8 [15]. The average absolute deviation is equal to 1.38%.

F. Validation of Chemical Parameters

The electrolyte solution chemistry has been modeled by specifying all the reactions involved in the process.

All reactions are assumed to be in chemical equilibrium except the reactions of CO_2 with OH^-.

$CO_2 + 2H_2O \leftrightarrow HCO_3^- + H_3O^+$	Equilibrium	(R.1)
$2H_2O \leftrightarrow OH^- + H_3O^+$	Equilibrium	(R.2)
$H_2O + HCO_3^- \leftrightarrow CO_3^{2-} + H_3O^+$	Equilibrium	(R.3)
$H_2O + H_2S \leftrightarrow HS^- + H_3O^+$	Equilibrium	(R.4)
$H_2O + HS^- \leftrightarrow S^{2-} + H_3O^+$	Equilibrium	(R.5)
$H_2S + OH^- \leftrightarrow HS^- + H_2O$	Equilibrium	(R.6)
$HS^- + OH^- \leftrightarrow S^{2-} + H_2O$	Equilibrium	(R.7)
$NaOH \rightarrow Na^+ + OH^-$	Dissociation	(R.8)
$Na_2CO_3 \rightarrow 2Na^+ + CO_3^{2-}$	Dissociation	(R.9)
$NaHCO_3 \rightarrow HCO_3^- + Na^+$	Dissociation	(R.10)
$Na_2S \rightarrow S^{2-} + 2Na^+$	Dissociation	(R.11)
$CO_2 + OH^- \rightarrow HCO_3^-$	Kinetic	(R.12)
$HCO_3^- \rightarrow CO_2 + OH^-$	Kinetic	(R.13)

The reactions defined in Aspen Plus™ are presented in the following expressions. Chemical equilibrium constants for the instantaneous reversible reactions are calculated using the following expression employed by Aspen Plus™:

$$\ln K_{eq} = A + \frac{B}{T} + C \ln T \qquad (5)$$

The calculation of the temperature-dependent equilibrium constants requires the knowledge of coefficients A, B and C which were taken from [16] Coefficients used for reactions (R.1) to (R.5) are presented in Table III. Those coefficients are unavailable in literature for reactions (R.6) and (R.7). Therefore, equilibrium constants of those two reactions were calculated by Aspen Plus™ using Gibbs free energies.

TABLE III
COEFFICIENTS USED IN THE CALCULATION OF THE EQUILIBRIUM CONSTANT

Reaction	A	B	C
R.1	231.465	-12092.1	-36.7816
R.2	132.899	-13445.9	-22.4773
R.3	216.05	-12431.7	-35.4819
R.4	214.582	-12995.4	-33.55471
R.5	-9.74	-8585.47	0

Results for reaction (R.6) were verified using equilibrium constants of reactions (R.2) and (R.4) by using expression (6). Fig. 9 shows the results obtained.

$$K_{eq,R.6} = \frac{K_{eq,R.4}}{K_{eq,R.2}} \qquad (6)$$

A temperature-dependent expression was proposed in order to define coefficients A, B and C for reaction (R.6). The values of the defined coefficients are presented in Table IV.

TABLE IV
COEFFICIENTS USED IN THE CALCULATION OF THE EQUILIBRIUM CONSTANT

Reaction	A	B	C
R.6	147	-1930	-21.15

The same method has been adopted in order to validate the equilibrium constant for reaction (R.7). For kinetic-controlled reactions (R.12) and (R.13), the power law expression (7) is adopted by Aspen Plus™:

$$r = kT^n e^{\left(\frac{-E}{RT}\right)} \prod_{i=1}^{N} C_i^{a_i} \qquad (7)$$

where r is the rate of reaction, k is a pre-exponential factor, T is the temperature, n is a temperature exponent, E is the activation energy, R is the universal gas constant, C_i is the concentration of component i and a_i is the stoichiometric coefficient of component i in the reaction. The concentration is based on molarity, the factor n is equal to zero, k and E parameters are given in the Table V for reactions (R.12) and (R.13). The kinetic parameters are taken from [17].

TABLE V
PARAMETERS K AND E FOR KINETIC-CONTROLLED REACTIONS

Reaction	k	E [cal/mol]
R.12	4.32E+13	13249
R.13	2.83E+17	29451

The reaction rate constants for the kinetic reaction between CO_2 and OH^- have been verified against experimental data [18]. Fig. 10 shows the good agreement of the results. The average absolute deviation is equal to 0.78%.
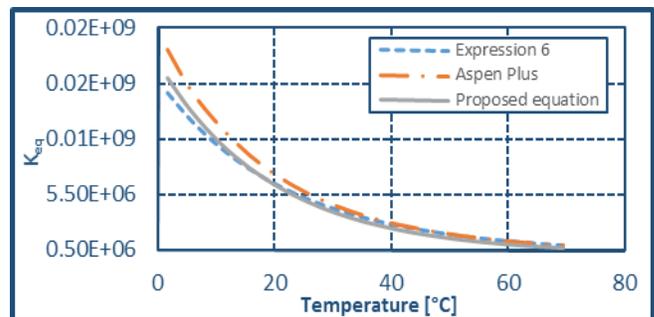

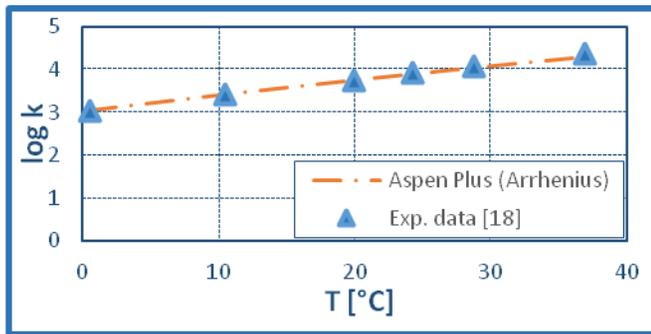Fig. 9 Comparison of results of equilibrium constant for reaction R.6

Fig. 10 Comparison of results of reaction rate constant for reaction R.12

G. Simulation Results

After validation of physicochemical parameters, Aspen Plus™ simulations for the packed absorption column of the pilot plant have been performed using the Rate-based model.

Details of the column used in the experiments, as well as the description of the given gas and liquid inlets are defined in Table VI.

When designing a packed column, it is desired to minimize the flow of liquid to reduce the consumption of water and the energy needed by the pump for its circulation. However, the flow must allow the absorption of H_2S and reduce its content to less than 1 ppm. This is a very important parameter since it has an influence on the thermodynamic and hydrodynamic conditions.

TABLE VI
DETAILS OF THE SIMULATED PROCESS

Packed column	
Diameter	0.15 m
Type of packing / Size / Material / Vendor	Flexipac 500Y Metal KOCH
Packing height	2.354 m
Gas inlet	
Temperature	9 °C
Pressure	1 atm
Mass flow rate	90 kg/h
Volume flow rate	77 m3/h
Molar composition	CH_4 (60%) CO_2 (39.997 %) H_2S (30 ppm)
Liquid inlet	
Temperature	4 °C
Pressure	1 atm
Mass flow rate	420 kg/h
Composition	Water with NaOH (0.5 g/L)

Sanchez et al. showed that with a fixed air flow, an increase in liquid flow rate will improve the velocity of transfer [19]. Fig. 11 is obtained using Aspen Plus™ demonstrates that increasing the liquid flow improves the absorption of H_2S. However, a mass flow rate of 240 kg/h is sufficient to eliminate the totality of H_2S with a minimal pressure loss.

As shown in Fig. 11, chemical conditions strongly influence the transfer percentage. The absorption rate increases with the concentration of NaOH in the liquid phase.
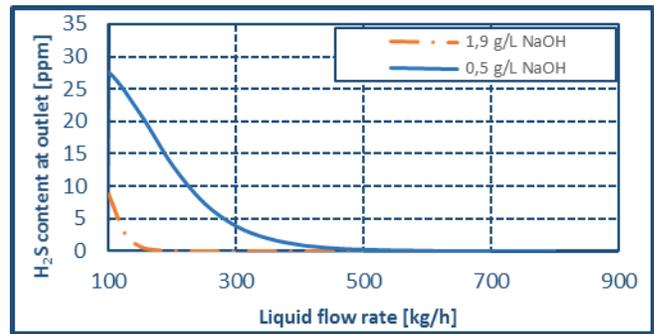

Fig. 11 Influence of the liquid flow on the absorption of H_2S

Fig. 12 shows that the increase in liquid flow causes a rise in pressure drop. This increase is limited, and shows that this parameter does not depend too much on the liquid flow. The results obtained on the pilot plant were compared to those from a calculation code made starting from the Billet and Schultes model [20]. It allows the calculation of hydrodynamic parameters as pressure drop, liquid holdup, effective interfacial area and mass transfer coefficients. The modified model based on semi-empirical correlations was tested and validated with experimental data from literature [20].
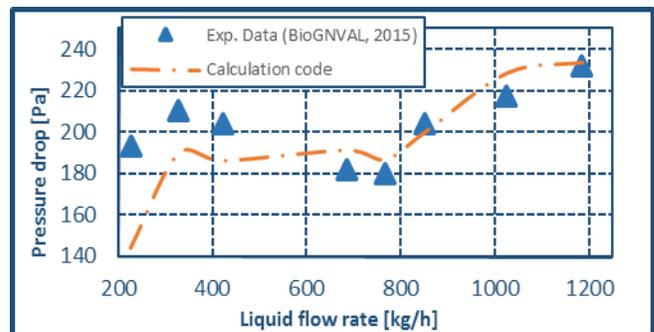

Fig. 12 Influence of liquid flow rate on the pressure drop

The dependence between the pressure drop and the gas flow rate is much more important as shown in Fig. 13, because the gas has the continuous phase in the packed column.
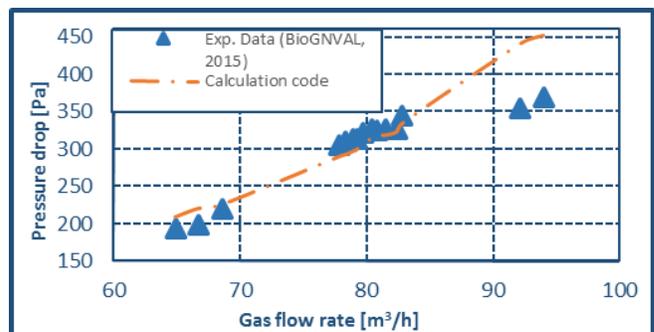

Fig. 13 Influence of gas flow rate on the pressure drop

A key parameter affecting the overall performances of the absorption unit is the temperature, since it affects physicochemical properties (such as the solubility of acidic

compounds in the aqueous phase, according to the Henry's law) and the chemical reactions in the liquid phase. Fig. 14 shows a good agreement between the results of Aspen Plus™ simulations and those obtained from the pilot plant.
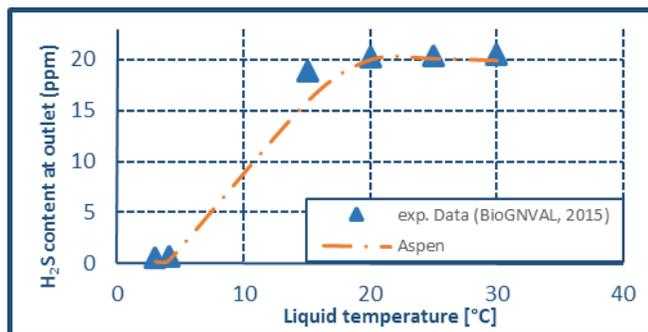

Fig. 14 Influence of the temperature of liquid in the absorption of H_2S

IV. CONCLUSION

The thermodynamic model used in the simulations (Electrolyte NRTL) was validated with experimental data from the literature.

Simulations were performed in order to study the influence of temperatures, chemical and hydrodynamic parameters on H_2S absorption. The simulation results were compared to experimental data obtained on the BioGNVAL pilot plant. The comparison was successful and shows that the two results are in good agreement. The model allows predicting realistically the separation efficiencies of H_2S in biogas.

REFERENCES

[1] Paul Benkimoun and Sophie Landrin, "Diesel: 42000 morts prématurées chaque année en France", Journal le monde 02/03/2013 according to the Ministry of Ecology, France.
[2] Encyclopédie des Gaz, Air Liquide – Pages : 1019 – 1052.
[3] CryoPur R&D society, 3, Rue de la croix martre, 91120 Palaiseau, France.
[4] Arthur Kohl and Richard Nielsen, "Gas purification, fifth edition", 331-402, (1997).
[5] Taylor, R., R. Krishna, and H. Kooijman, "Real-World Modeling of Distillation," Chem. Eng. Prog., (July 2003), 28-39.
[6] Chau-Chyun Chen, David Tremblay, Chai Bhat, A Rate-Based Process Modeling Study of CO_2 Capture with Aqueous Amine Solutions using aspenONE Process Engineering (June 2008).
[7] Chau-Chyun Chen and Yuhua Song Generalized electrolyte-NRTL model for mixed-solvent electrolyte systems, American Institute of Chemical Engineers AIChE J, 50: 1928–1941, (July 2004).
[8] Gillespie, P. C. and G. M. Wilson, Gas Processors Association, Research Report RR-48, (April 1982)
[9] Harvey, A. H., AIChE J. 42, 1491, (1996).
[10] J. R. Elliott and C. T. Lira, Prentice-Hall Introductory Chemical Engineering Thermodynamics, (1999).
[11] N.M. Herrington, A.D. Pethybridge, M.G. Roffey, "Densities of Aqueous Lithium, Sodium, and Potassium Hydroxides From 25 to 75 C at 1 Atm", J. Chem. Eng. Data, 31, 31-34(1986)
[12] Z. Palaty, Viscosity of diluted aqueous $K_2CO_3/KHCO_3$ solutions, Collect. Czech. Chem. Commun., 57, 1879 (1992).
[13] J.S. Pac, I.N. Maksimova, L.V. Glushenko, Viscosity of alkali salt solutions and comparative calculation method, J. Appl. Chem. USSR., 57, 846 (1984).
[14] N.B. Vargaftik, Dictionary of thermophysical properties of gases and liquids, Moskva (1972).
[15] N.I. Gel'perin, B.M. Gurovich, K.K. Dubinchik, The relation between the surface tension of aqueous solutions of inorganic substances and concentration and temperature, J. Appl. Chem. USSR, 42, 190-192 (1969).
[16] T.J. Edwards, G. Maurer, J. Newman, J.M. Prausnitz, AIChE J. 24 1978. 966–976.
[17] B.R. Pinsent, L. Pearson, F.J.W. Roughton, The kinetics of combination of carbon dioxide with hydroxide ions", Trans. Faraday Soc., 52, 1512-1520 (1956).
[18] Faurholt, C., J. chim. physique, 21, 490 (1925).
[19] C. Sanchez, A. Couvert, A. Laplanche, C. Renner, Hydrodynamic and mass transfer in a new concurrent two-phase flow gas-liquid contactor, Chemical Engineering Journal, 131, (1-3) 49-58 (2007).
[20] André Brink Erasmus, Mass transfer in structured packing Department of Process Engineering, University of Stellenbosch, January (2004).